11-30-2015

Simple modification of Compton polarimeter to redirect synchrotron radiation

J. Benesch
Thomas Jefferson National Accelerator Facility

Gregg Franklin
Carnegie Mellon University, gbfranklin@cmu.edu

Brian Quinn
Carnegie Mellon University, bquinn@cmu.edu

K. D. Paschke
University of Virginia

Published In
Physical Review Special Topics: Accelerators and Beams, 18, 112401.

Simple modification of Compton polarimeter to redirect synchrotron radiation

J. Benesch
Thomas Jefferson National Accelerator Facility, Newport News, Virginia 23606, USA

G. B. Franklin and B. P. Quinn
Carnegie Mellon University, Pittsburgh, Pennsylvania 15213, USA

K. D. Paschke
University of Virginia, Charlottesville, Virginia, 22903, USA

(Received 17 March 2014; revised manuscript received 17 August 2015; published 30 November 2015)

Synchrotron radiation produced as an electron beam passes through a bending magnet is a significant source of background in many experiments. Using modeling, we show that simple modifications of the magnet geometry can reduce this background by orders of magnitude in some circumstances. Specifically, we examine possible modifications of the four dipole magnets used in Jefferson Lab's Hall A Compton polarimeter chicane. This Compton polarimeter has been a crucial part of experiments with polarized beams and the next generation of experiments will utilize increased beam energies, up to 11 GeV, requiring a corresponding increase in Compton dipole field to 1.5 T. In consequence, the synchrotron radiation (SR) from the dipole chicane will be greatly increased. Three possible modifications of the chicane dipoles are studied; each design moves about 2% of the integrated bending field to provide a gentle bend in critical regions along the beam trajectory which, in turn, greatly reduces the synchrotron radiation within the acceptance of the Compton polarimeter photon detector. Each of the modifications studied also softens the SR energy spectrum at the detector sufficiently to allow shielding with 5 mm of lead. Simulations show that these designs are each capable of reducing the background signal due to SR by three orders of magnitude. The three designs considered vary in their need for vacuum vessel changes and in their effectiveness.

DOI: 10.1103/PhysRevSTAB.18.112401 PACS numbers: 29.20.Ej, 29.27.Eg, 29.27.Hj

I. INTRODUCTION

The total energy of the synchrotron radiation produced by an electron following an arc of constant radius r as it is bent through an angle $\Delta\theta$ is (see, for example, Ref. [1])

$$\frac{dE}{d\theta}\Delta\theta = \frac{2}{3}\alpha\frac{\hbar c}{r}\gamma^4\Delta\theta. \tag{1}$$

The synchrotron radiation has an angular dependence given by a leading term of the form $[1+(\gamma\theta)^2]^{-3}$, where $\gamma = E/(mc^2)$ is the Lorentz factor determined by the electron beam energy E and electron mass m. Because of the typically high Lorentz factor γ, the synchrotron radiation is emitted in a very narrow cone centered along the trajectory of the electron. Thus the most troublesome synchrotron background usually comes from the radiation emitted at the exit of the last steering magnet upstream from a fixed target, or in the case of colliding beams such as the planned Electron-Ion Collider, the magnet used to direct the electron beam towards the intersection point. In some cases, such as the Compton polarimeter discussed below, the entrance to the first steering magnet after the target generates an additional source of synchrotron background.

The mean number of photons emitted as the electron is bent through an angle $\Delta\theta$ can be written as

$$\frac{d^2N_\gamma}{dE_\gamma d\theta} = \frac{\sqrt{3}}{2\pi}\frac{\alpha\gamma}{E_c}\int_{E_\gamma/E_c}^{\infty} K_{5/3}(x)dx, \tag{2}$$

where $K_{5/3}$ is the modified Bessel function of the third kind, α is the fine structure constant and E_c is a characteristic energy given by:

$$E_c = \frac{3\hbar c}{2r}\gamma^3. \tag{3}$$

For a nonuniform magnetic field, r is the local bending radius of the electron's trajectory, $r = p/(eB_\perp)$.

The energy scale for the instantaneous synchrotron spectrum is set by E_c, with exactly half the photons having energies above E_c. The spectral shape is a universal function of E_γ/E_c. The factor of γ^3 in (3) indicates that

the gamma-ray spectrum becomes much harder as γ increases. That factor combines with the additional factor of γ in (2) to give a γ^4 dependence to the total synchrotron radiation power as expressed in (1). This can be mitigated by increasing the bending radius r by implementing a design which features a reduced local magnetic field in critical regions, as discussed below.

In this paper, we show that a dipole design employing floating pole-face extensions specifically designed to create a spatially extended fringe field can be used to reduce synchrotron radiation hardness and to decrease the integrated radiated energy by orders of magnitude. Although the concepts are general, the implementation will be site-specific. The modeling of the Jefferson Lab Hall A Compton polarimeter, discussed below, serves as a specific example of the potential background reduction that can be achieved using this approach. While suitable low-field regions could, in some situations, be achieved by introducing additional dipoles, the implementation of the designs discussed below are relatively inexpensive, require no additional power supplies, fit into contained spaces, are easily customized to work around obstacles, and are self-scaling with the dipole field.

II. THE HALL A COMPTON POLARIMETER

A Compton polarimeter relies on the Compton scattering of polarized laser photons by polarized electrons. The Compton cross section depends on the relative orientation of the photon spin and the electron spin. Since these cross sections can be calculated from first principles, a measured asymmetry A_{measured} of the scattering rates between positive-helicity electron bins and negative-helicity electron bins for a fixed photon polarization can be used to determine the polarization of the electron beam through the relation $A_{\text{measured}} = P_{\text{beam}} P_{\text{photon}} A_{\text{Compton}}$, where P_{beam} is the unknown beam polarization, P_{photon} is the known photon polarization, and A_{Compton} is the theoretical Compton cross section asymmetry. At Jefferson Lab, the beam polarization is typically around $P_{\text{beam}} = 90\%$ and the Compton polarimeter can measure the actual value of P_{beam} to better than 1%.

The Hall A polarimeter is shown schematically in Fig. 1 and is described in [2]. When the Compton polarimeter is in use, the beam is steered through a chicane of four 1-meter dipoles, labeled D1 through D4, so that it passes through a Fabry-Perot cavity where it can scatter off polarized photons. About 1 in 10^9 electrons interact with the photons so the polarimeter may be operated on a full current beam. The spin-dependent Compton scattering asymmetry, A_{measured}, can be measured using either a photon detector located downstream of dipole D3 or an electron detector (not shown) located above the beam downstream of D3. As shown in Fig. 1, the photon detector sees the synchrotron radiation produced as the beam exits D2 and as it enters D3.

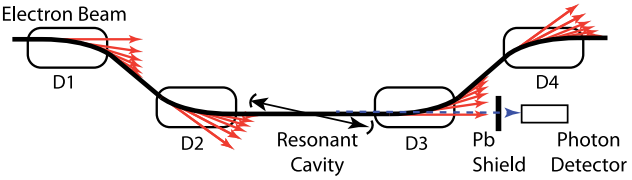

FIG. 1. Hall A Compton polarimeter. Fan-shaped regions qualitatively represent synchrotron radiation.

JLab's energy-upgrade projects necessitated several modifications to the polarimeter. Prior to the upgrade, the chicane magnets were installed with a vertical drop of 30.4 cm to the scattering location. This was decreased to 22 cm in 2013 to keep the field in the dipoles within their rated value of 1.5 T when running with an 11 GeV beam.

In anticipation of future running, detailed modeling of the synchrotron radiation background was performed. Two-dimensional magnet modeling was done using Poisson and the resulting field was used to determine the corresponding synchrotron energy spectrum given by (2), as discussed in more detail in Sec. IV.

The results of this modeling are shown in Fig. 2. The synchrotron radiation spectra in the Compton photon detector, modeled for conditions during two completed experiments, HAPPEX III [3] and PVDIS [4], are compared to the spectrum obtained from modeling the 1.5 T dipoles in their new location and an 11 GeV beam. The effects of thin lead filters in front of the photon detector are shown in dashed lines of the same color as the primary spectra. Thin filters for synchrotron radiation (SR) are preferred to avoid attenuation or showering of the Compton-scattered photon flux which would reduce the precision of the analyzing power calibration. In particular, techniques using an integration of photon signals over

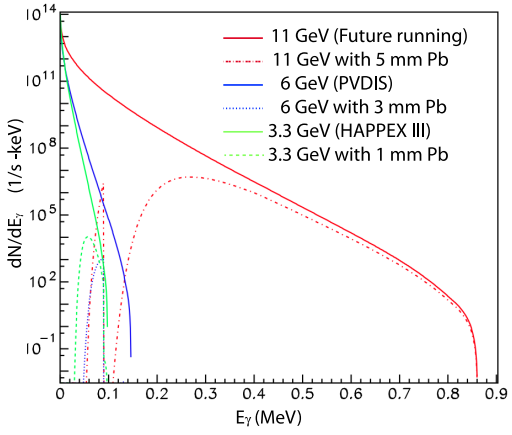

FIG. 2. Comparison of the synchrotron radiation from a 100 μA electron beam produced within the acceptance of the Compton polarimeter's photon detector, for two completed experiments, PVDIS at 6 GeV and HAPPEX III at 3.3 GeV with the repositioned 11 GeV Compton system. The dashed/dotted lines show the effect of thin lead filters.

fixed periods of time [5], which avoid significant systematic uncertainties in calibrating the effects of a trigger threshold, require well-understood detector response even to low energies in the Compton spectrum. While the Compton spectrum is boosted to higher energy with higher beam energy (up to a few GeV for 11 GeV beam operation, compared to 600 MeV for 6 GeV beam), the energy endpoint and intensity of the SR spectrum rises more quickly.

Recent operation at an electron beam energy of 6 GeV [4] showed a marked reduction in the polarimeter precision due to the need for thicker shielding. The filters were sufficient in the lower-energy cases but even 5 mm would allow far too many moderate energy photons through when running an 11 GeV beam, illustrating the need for reducing the SR flux incident on the photon detector through another technique.

III. MODELING OF DIPOLES WITH FIELD EXTENSIONS

Additional 2D analysis suggested that a 400 G field within 60 cm long regions after the second dipole and before the third would bend the beam before and after the interaction-point in a manner which would minimize the synchrotron radiation within the acceptance of the photon detector. This was impractically long and 2D analysis is not appropriate for dealing with the end of a dipole. Additional modeling was performed using OPERA [6]. To obtain an accurate model of the existing chicane dipoles, the current density in the model was iterated until the integrated field on a circular orbit corresponding to a hard-edged dipole was within 0.01% of that needed for beam transport through the Compton chicane. This current density was used for all models.

A trajectory approximated as a circular orbit was used for evaluating all models until the final step. The circular path used is normal to the face of the third dipole and 1.02 cm below the middle of the pole exiting the interaction region. Some hundred variations were evaluated, with SR spectrum and the effects of lead filters calculated for zero emittance beams. The coils in the models shown have a smaller envelope, but the same center of gravity as the real coils since OPERA works best if there is an air gap of at least one voxel layer between coil and magnetic material [7].

Three classes of variations on the original dipole design (denoted Class R, Class RF, and Class RS) are considered here. The first class of designs, denoted Class R, considered variations based on a simple rectangular plate, 10 cm wide by 11 cm long and 2.5 cm thick, to extend the field. The existing dipole coil location results in a plate separation of 5.5 cm. An example of a Class-R design is shown in Fig. 3. The rectangular plate, shown in blue, fits entirely inside the coils so no modification to the vacuum vessel is needed and this is therefore the lowest-cost solution.

The second class is represented by a much more complicated model, as shown in Fig. 4. This class of designs,

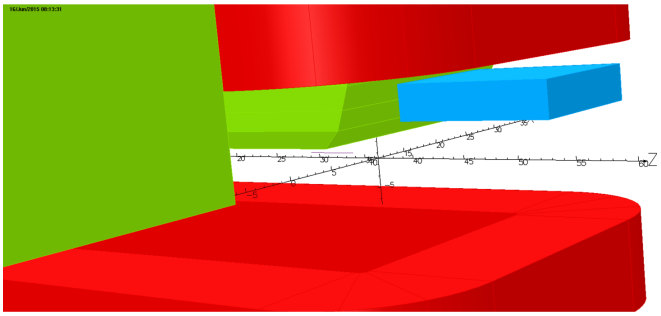

FIG. 3. Example of a Class-R field-extension design: a single rectangular plate 10 cm by 11 cm. The magnet yoke and main pole piece are shown in green, the coils in red, and the field extension component in blue.

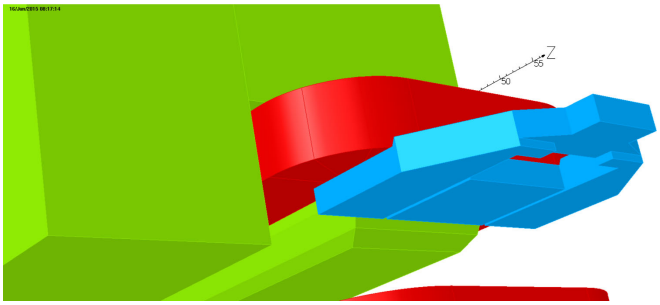

FIG. 4. Example of a Class-RF design: a rectangular extension combined with an additional forked component.

based on a rectangular plate in conjunction with a fork, is denoted Class RF. The field extension components consist of two parts: a rectangular plate and a large fork, which allows it to be fitted around an existing 15 cm diameter pair of vacuum flanges. The fork moves flux out to larger z (distance from dipole center). This produces more bending with low field and thus a softer synchrotron radiation spectrum at the Compton photon detector. The width of the gaps between the small plate and the fork is very important in maintaining optimal flux in each region. Models with 2, 5, 10, and 20 mm gaps were tried; 5 mm was the best of these. The increase in plate spacing at the end accommodates an existing gate valve. The rectangular hole allows for installation with the 15 cm CF flanges and bolts.

An example of the third class of field-extension designs is illustrated in Fig. 5. This class of designs, based on a combination of the rectangular plate and a tapered and stepped component, is denoted Class RS. These designs include a wide plate (full pole width) between the coils, a step out to 7.1 cm separation to accommodate rectangular vacuum flanges, and a piece tapering to 8 cm to concentrate flux and keep the field up where the beam will pass. The beam enters the magnet 1 cm off axis to minimize multipoles in the dipole proper. The width of the tapered end, 8 cm, is a compromise between field quality and quantity between the plates, one of the variables explored in over

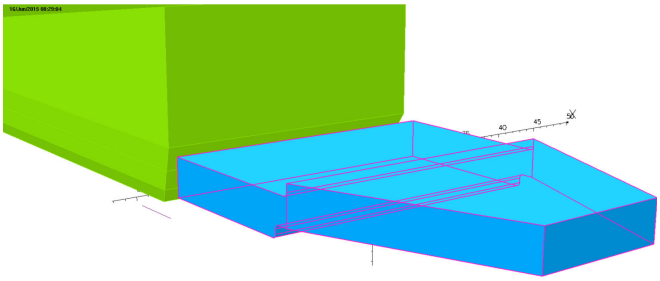

FIG. 5. Example of a Class-RS design shown with coils suppressed. In addition to the rectangular plate, the design uses a step up to a tapered component which concentrates the flux and therefore increases the field in the region with larger gap.

100 model variations. The plate separation was set to accommodate flanges matching the bonnet flanges on VAT all-metal vacuum gate valves used in the Hall C Compton chicane. A flange width of 70 mm was used in that polarimeter and assumed in our design for this option.

The iteration process required many plots like those in Figs. 2 and 6. One wants ∼30 kG-cm of bending with as uniform and low a field as possible at the D2 exit and D3 entrance regions to soften the synchrotron radiation spectrum within the aperture of the Compton photon detector. The stepped-taper plate design, Class RS, is closest to this ideal, extending significant field strength more than 25 cm. beyond the edge of the magnet (at 50 cm from the center) and having extended "plateaus" of 1600 G and 1200 G.

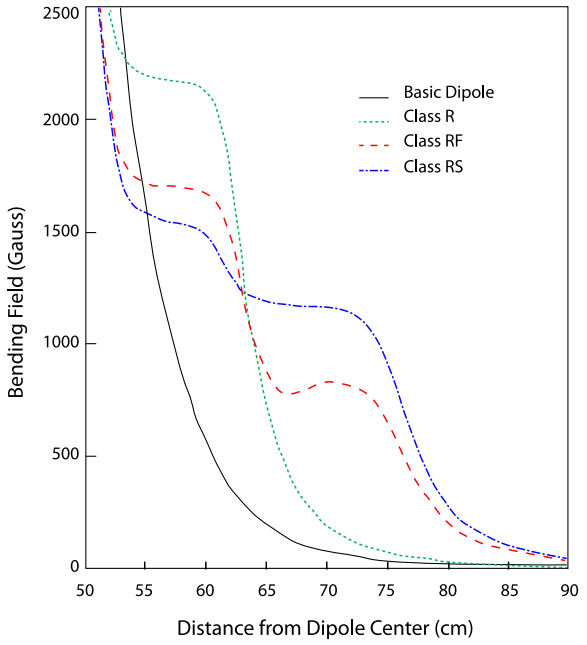

FIG. 6. Bending fields along the circular arc for the four models discussed above. The field values for the three classes of extensions have been normalized to give the same integral of BdL along the approximate beam path. For example, the larger bending field of Class-RS fringe field compared to the basic dipole is compensated by a slightly lower central field.

The rectangle plus fork design, Class RF, shows that a solution is possible even if one must work around existing vacuum components. Designs based on a simple rectangular plate extension, Class R, are the simplest but least effective.

IV. EVALUATION OF SYNCHROTRON RADIATION SPECTRUM

The energy spectrum of synchrotron photons expected to reach the photon detector was found by numerical integration of the flux expected to pass through a 6.0 mm hole in a lead collimator positioned just upstream of the photon detector. The collimator is 575 cm downstream from the center of the Compton cavity, so it is 460 cm away from the entrance face of dipole D3 and 625 cm from the exit face of dipole D2 (see Fig. 1). Because of the high relativistic γ, the simulated synchrotron radiation photons were simply modeled as being produced at zero degrees with respect to the electron trajectory.

The integration followed an electron (assumed to be moving horizontally at the center of the cavity) as it entered the magnetic field associated with dipole D3. For each step, the new position and direction of the electron were calculated and the expected spectrum of synchrotron radiation emitted in that step was added to a running-sum spectrum. This was continued until the deflection of the electron was large enough that the radiation would no longer pass through the collimator aperture. Similarly, the contribution from the beam exiting dipole D2 was found by following an electron in negative time steps from the Compton cavity to the point where its deflection would have been large enough that its radiation would not have passed through the aperture. Stable results for the predicted total spectrum were obtained for step sizes anywhere from 0.1 to 1.0 mm. The effect of thin lead filters on very low energy photons was included by modeling the photon attenuation length as being entirely due to photon absorption. This correctly modeled the rapid variations in shielding effect at wavelengths corresponding to x-ray resonances.

This effect is demonstrated in Fig. 7, which compares the expected synchrotron radiation flux at the Compton photon detector for a 100 μA beam of 11 GeV electrons deflected by unmodified dipoles and by three variations designed to introduce low field in the relevant regions. The Class-RS design is seen to greatly reduce the photon flux compared to the basic dipole. Furthermore, it softens the photon spectrum so that a thin lead filter, which is very effective for photon energies up to about 0.25 MeV, will eliminate most of the flux.

Additional studies were done, summarized in Fig. 8, to examine the sensitivity of the reduction in the integrated SR power to misalignment of the electron beam relative to the collimator. Comparison of the points at vertical offset equal to zero (beam aligned with the collimator) demonstrates the reduction in SR power by three (or more) orders of

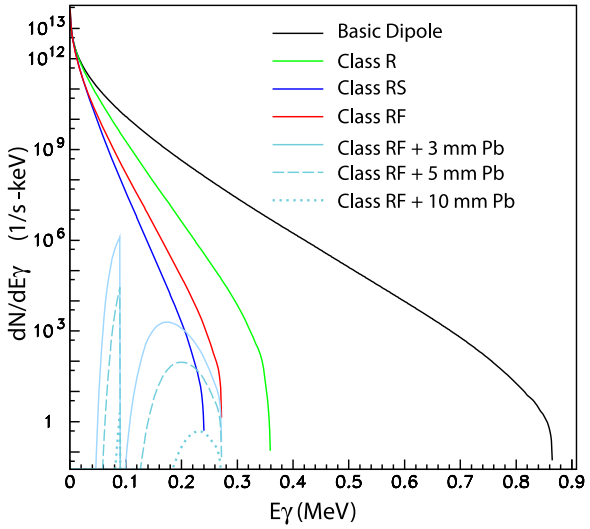

FIG. 7. Synchrotron-radiation spectra from a 100 μA electron beam for the basic Compton dipole (black) and for an example of each of the three class variations For the Class-RF example, the effects of three thicknesses of lead filters are also shown.

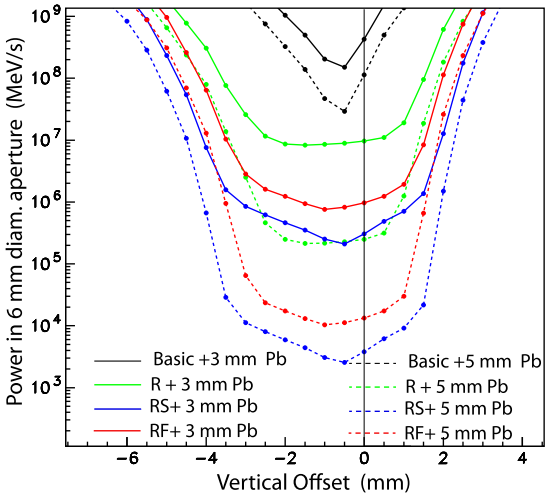

FIG. 8. The effect of possible electron-beam misalignment is shown by plotting power of the synchrotron radiation entering a 6-mm-diameter collimator as a function of vertical beam position. A 100 μA beam is assumed.

magnitude for a Class-RS design compared to the basic dipole. These results also served as a rough estimate of sensitivity to beam divergence and angular spread of the radiation, both of which were neglected. As shown in the figure, an upward displacement of the collimator of 1.5 to 2 mm with respect to the electron beam resulted in little increase in flux for the Class-RS and Class-RF designs. These modifications were even more tolerant of downward displacements of the collimator because of the longer lever arm between D2 and the collimator. This results in greater displacement of the radiation from the downward-going electron beam in the high-field region at the exit of dipole D2. This safety margin indicates that small angular spreads of the beam and radiation would not result in catastrophic increase in the flux at the photon detector.

V. HIGHER FIELD MULTIPOLES

Most of the parameter space was explored with models which assumed symmetry about the $z = 0$ and $y = 0$ planes. After a specific model for each of the three design classes was chosen, the OPERA models were rebuilt without assuming symmetry about $z = 0$, roughly doubling the size of the models. In all the models the mesh size for the added plate was set at 5 mm. The pole of the dipole proper, which extends from $z = -50$ cm to $z = 50$ cm, was also meshed at 5 mm. The air in the volume $x = [-3, 3]$ cm, $y = [0, 1.27]$ cm, $z = [-80, 80]$ cm was meshed at 2.5 mm for the basic dipole. For models with steel plates, the finer mesh volume was extended to $z = -90$ cm. "Quadratic elements," which create quadratic interpolation formulas at each node, were used except at large distances from the magnet steel. The 2.5 mm mesh size for the "beam air" is driven by the sampling theorem. Multipoles are calculated on 1 cm radius circles along the beam path. There are ~25 samples at 2.5 mm intervals on a 1 cm radius circle. As expected from Shannon's sampling theorem, previous unpublished studies by one of the authors (J.B.) confirmed that this suffices for multipoles up to $n = 5$ (sixth harmonic) and provides some information up to $n = 9$ (tenth harmonic).

Multipoles may be computed in OPERA in two ways analogous to laboratory measurements. One may obtain integrated fields on straight lines or arcs of circles (better) at, say, 2 mm intervals, and fit parabolas to these. One may then read off dipole, quadrupole and sextupole terms from the coefficients of the fit. Doing this with straight lines is analogous to stretched wire measurements.

The "moles" used by superconducting magnet laboratories have coils wound to intercept particular multipoles and a single rotating wire to pick up the total field [8]. The measured multipoles are subtracted from the single-wire measurement to evaluate the higher multipoles. In OPERA one may launch a particle and obtain the orbit parameters from an output file. The orbit parameters (x, y, z) may then be used to specify the centers of circles upon which a field component, By, is calculated at a chosen number of points. OPERA's post-processor has a "fit Fourier" command which does just that, for a user-chosen number of harmonics. These are designated Cos0 (dipole) to Cos4 (decapole), for example, in the POST output. These results are then extracted from the text output file for further analysis and plotting. The circles used for multipole calculation must be normal to the z axis, not the orbit, to avoid the inclusion of a geometric term resulting from the wedge-shaped areas between the circles. This may be verified by comparison with the multipole values obtained from the fitted parabolas. Multipoles along particle orbits launched at $x = 1$,

TABLE I. Multipole values along particle orbits for five modeled dipoles.

Dipole model	Dipole Cos0	Quadrupole Cos1	Sextupole Cos2	Octupole Cos3	Decapole Cos4
Hall A arc	−2751316	−148.3	180.4	−15.5	−2.3
Basic Compton	−1496124	−19.3	98.9	3.3	1.8
Class R	−1504444	−59.5	118.0	−9.5	14.1
Class RS	−1504990	−65.3	127.4	−8.8	0.5
Class RF	−1501289	11.0	93.4	0.4	−3.7

$y = 0$, $z = -120$ cm for the basic dipole and three modifications discussed here are given in Table 1.

Values for the Hall A arc dipole model are included in Table 1 for comparison; there are eight dipoles in the arc. The four Compton dipole models have the same current density. Particle energies were scaled by dipole BdL (Cos0 in table) so the orbit would end at the same location and angle. The quadrupoles and sextupoles in the beam line leading to Hall A from the CEBAF accelerator may be adjusted to deal with the differences shown. Octupole and decapole are not significant for a fixed target machine. Note that the basic Compton dipoles are of equal or better quality (lower multipoles) than the eight dipoles in the Hall A arc. If the magnets were H core rather than C core the changes in octupole and decapole at the few ppm level due to the steel extensions would not be significant for a storage ring fitted with correction magnets of the respective types. Quadrupole and sextupole changes would have to be taken into account in design or modification of a storage ring with such extensions.

For a magnetic chicane, the four dipoles should be closely matched but it is not necessary to use the same extensions on all four dipoles. For example, to reduce cost Class-R-style extensions, which do not require vacuum flange changes, could be used for the first and fourth dipoles while Class-RS-style extensions could still be used on the second and third dipoles since these are the only dipoles which project synchrotron radiation into the Compton photon detector. In this case, the thickness of the Class-R extensions could be increased to better match the BdL effect of the Class-RS-style extensions over the full range of beam energies. The dipoles have a 2% trim winding which could be used to compensate for any steering due to imperfections in the dipole chicane.

VI. CONCLUSIONS

We have shown that a simple modification of the four dipoles in the Hall A polarimeter chicane, which moves about 2% of the integrated bending field, can be used to reduce the flux and energy of the synchrotron radiation within the acceptance of the Compton polarimeter photon detector by providing a gentle bend in the critical regions of the beam path. The increased bending radius lowers the SR energy spectrum at the detector sufficiently to allow shielding with 5 mm of lead, excluding the SR while allowing the Compton photons to reach the detector. These design changes will decrease the background signal due to synchrotron radiation by three orders of magnitude. This modification is inexpensive, with most of the incremental cost in the rectangular metal-sealed flanges.

ACKNOWLEDGMENTS

The Medium Energy Physics group at Carnegie Mellon University was supported by DOE Grant No. DE-FG02-87ER40315. Work at University of Virginia was supported by DOE Grant No. DE-FG02-07ER41522. One author (J. B.) was employed by Jefferson Science Associates, LLC under U.S. DOE Contract No. DE-AC05-06OR23177 during the course of this work.

[1] J. D. Jackson, *Classical Electrodynamics* (Wiley & Sons, New York, 1975).
[2] N. Falletto *et al.* (HAPPEX Collaboration), Compton scattering off polarized electrons with a high finesse Fabry-Perot cavity at JLab, Nucl. Instrum. Methods Phys. Res., Sect. A **459**, 412 (2001).
[3] S. Abrahamyan *et al.* (PREX Collaboration), Measurement of the Neutron Radius of ^{208}Pb Through Parity Violation in Electron Scattering, Phys. Rev. Lett. **108**, 112502 (2012).
[4] D. Wang *et al.* (Jefferson Lab Hall A Collaboration), Measurements of Parity-Violating Asymmetries in Electron-Deuteron Scattering in the Nucleon Resonance Region, Phys. Rev. Lett. **111**, 082501 (2013).
[5] M. Friend, D. Parno, F. Benmokhtar, A. Camsonne *et al.*, Upgraded photon calorimeter with integrating readout for the Hall A Compton Polarimeter at Jefferson Lab, Nucl. Instrum. Methods Phys. Res., Sect. A **676**, 96 (2012).
[6] http://cobham.vectorfields.com/.
[7] J. Benesch (private communication).
[8] E. Willen, P. Dahl, and J. Herrera, Superconducting Magnets, in *AIP Conference Proceedings 153*, edited by M. Month and M. Dienes, Physics of Particle Accelerators (American Institute of Physics, New York, 1987), pp. 1228.